

Sensitivity of a Frequency-Selective Electrode based on Spatial Spectral Properties of the Extracellular AP of Myelinated Nerve Fibers

Olivier Rossel Fabien Soulier Serge Bernard Guy Cathébras*

Abstract—In the context of functional electrical stimulation, neural recording is one of the main issues. For instance, the control of the limbs in people with motor deficiencies needs information about the muscle lengths and speeds that can be extracted from electroneurograms (ENG) carried on afferent peripheral nerves.

The aim of this study is to propose a non-invasive and spatial-selective electrode (because specific informations are carried into different fascicles). To do so, we investigate the spatial properties of an extracellular action potential (AP). These properties are described qualitatively and quantitatively using an analytical study on an inhomogeneous an anisotropic nerve model.

Then, a spectral analysis on this spatial signal discriminates the different frequency components. Low spatial frequencies represent the global shape of the signal, whereas high frequencies are related to the type of fibers. We show that the latter is rapidly attenuated with the distance and thus, being a local phenomenon, can be used as a selective measurement. Finally, we propose a spatial filtering based on electrode design and an electronic architecture to extract this high frequencies.

I. INTRODUCTION

In the context of functional electrical stimulation, neural recording is one of the main issues. For instance the control of the limbs in people with motor deficiencies needs information about the muscle length and speed [1] that can be extracted from the electroneurogram (ENG) carried on afferent peripheral nerves.

The ENG signals are recorded using electrodes, that is the interface between the nerve and the electronic amplifier. The main types of electrodes available are: cuff electrodes (flat or cylindrical), intrafascicular and sieves. Each kind has advantages and drawbacks, but for our application, we focus on the safety for the nerve and the selectivity of the electrode. By safety, at the electrode level, we mean the property of the electrode to be as non-invasive as possible for the nerve. The cuff electrode, being the least invasive, is our preferred choice. Because cuff electrodes are placed around the nerve, this study describes the electric field surrounding the nerve. This is calculated for one active axon in any place inside the nerve. Human tissues behave like a filter on biological signals which is described by a medium transfer function. It is essential to understand and quantify it in order to propose a custom acquisition system for peripheral ENG. The goal of this study is to find a local signal which could be extracted by a cuff electrode. In other words, we are looking for a characteristic signal generated by the closest axons.

All authors are with Laboratoire d'Informatique de Robotique et de Microélectronique de Montpellier, 161 rue Ada, 34392 Montpellier, France Université Montpellier II — CNRS — INRIA — INSERM

*Firstname.Lastname@lirmm.fr

The propagation of neural signal along myelinated axons is due to the saltatory conduction. The action potential (AP) propagates along the axon from Nodes of Ranvier (NOR) to NOR. When an AP occurs, several NORs provide nodal current i_n at the same time. The conversion of the nodal current to electrical field is calculated using a transfer function description.

This paper first presents the spatial property of the AP. Then it explains the spectral properties of the AP. Thanks to a single AP study, a local phenomenon is described and a cuff electrode filtering is proposed to extract this local characteristic signal. Then combining the medium and electrode transfer function the total filtering is described. Finally the implementation of this kind of electrode is discussed.

II. SPATIAL PROPERTIES

We start by describing the spatial extracellular AP of an axon. This means that for one time instant, we are looking at the electrical activities along the axon, at a distance ρ' (the poles are located on the nerve surrounding, as presented in fig. 1). Using a simple model of the nerve, the axons are modeled straight in the longitudinal axis, and the NOR are equally spaced with a distance of l_{my} (length of the myelin). The figure shows an example of a fiber of $8.7 \mu\text{m}$ diameter and 1 mm myelin length.

A. Discrete NoR Current

Here is presented the electrical activity of the active NORs of an axon. From the electrical shape of one NOR current $i_n(t)$ (ionic and capacitive, evaluated using NEURON software¹), and the electrical conductivity, the NOR current can be described as: $i_n(n, t) = i_n(t - nl_{my}/V)$, where V is the conduction velocity. The global shape of the spatial current ($i_n(n)$) is the shape of the nodal current ($i_n(t)$) reversed and dilated by the factor l_{my}/V . The NoR current can be described as the global shape current multiplied by Dirac comb (fig. 2.1a). Thus, in the space domain the NoR current is discrete: present where there are NoRs.

B. Medium Transfer Function

First, to facilitate the explanation, we present the extracellular AP calculation in a homogeneous and isotropic model. We considered the axon in an infinite conductive volume ($\sigma = 0.1 \Omega^{-1}\text{m}^{-1}$. (The conductivity of the nerve in each direction and the conductivity of the extraneurium are identical.) To describe the potential resulting from the simultaneous activation of successive nodes, we use linear

¹<http://www.neuron.yale.edu>

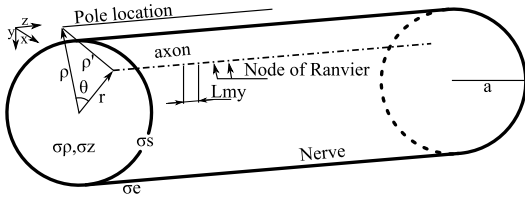


Fig. 1. Simple model of the nerve, the axon are modeled strait in the longitudinal axis, the NOR are equally spaced of a distance l_{my} length of the myelin. The spatial AP is observed on the nerv surrounding at a distance ρ'

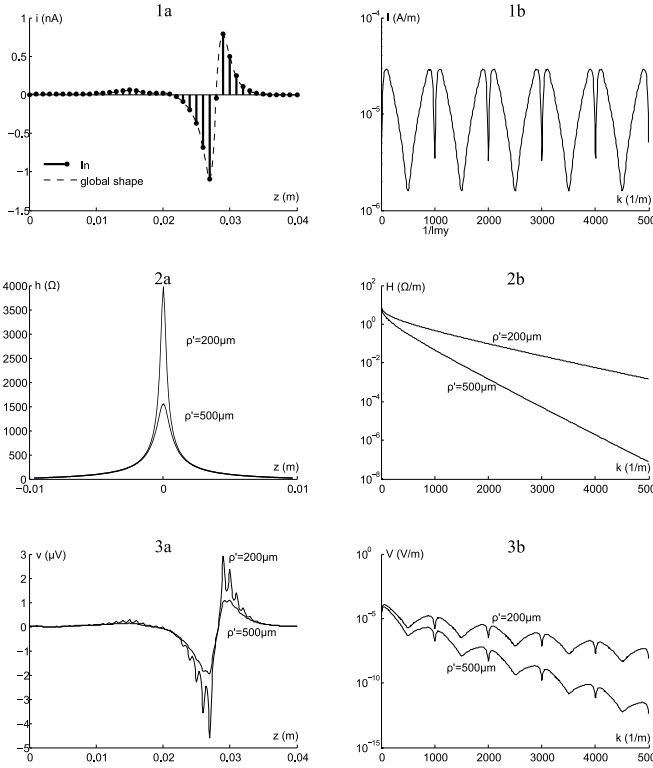


Fig. 2. 1a) spatial current. 1b) spatial current specter 2a) spatial transfer function 2b) spatial transfer function specter 3a) spatial AP along a single axon 3b) spatial AP specter (8.7 μm diameter and 1 mm of myelin length) at two distances: $\rho' = 200 \mu\text{m}$ and $\rho' = 500 \mu\text{m}$

superposition of potentials created by each node, so we can write

$$v(M) = \frac{1}{4\pi\sigma} \sum_n \frac{i_n}{\sqrt{\rho'^2 + (z - nl_{my})^2}}, \quad (1)$$

where i_n is the current flowing from node n , ρ' is the distance between the axon and the observation point M .

This equation can be written as a convolution product between the spatial NoR current $i_n(z)$ and the transfer function $h(z)$, so

$$v(M) = \underbrace{\frac{1}{4\pi\sigma} \frac{1}{\sqrt{\rho'^2 + z^2}}}_{h(z)} * \underbrace{\sum_n i_n \delta(z - nl_{my})}_{i_n(z)}. \quad (2)$$

This transfer function is represented in fig. 2.2a for two different distances ($\rho' = 200, 500 \mu\text{m}$). The amplitude and

smoothness of the transfer-function are linked to the axon depth. It is then analytically explained and quantitatively assessed with an anisotropic an inhomogeneous model.

C. Extracellular AP

On fig. 2.3a, the AP has the same global shape as the spatial current, but presents spikes resulting from the discretization of the spatial current. The position of each spike is related to the location of a NoR. Because the extracellular AP is the convolution product between the nodal-current and the transfer-function, it adopts the same behavior as the one of the transfer-function depending on the depth. As a result, the spikes amplitude decreases according to the axon depth.

III. SPECTRAL PROPERTIES

The right part of the fig. 2 presents the spectrum of the spatial signals discussed above. Their analytic expression will be detailed in the present section.

A. Discrete NoR Current

In the space domain, the current can be seen as a product between the nodal current global shape and a Dirac comb. In the frequency domain, it is the NoR current spectrum convoluted with Dirac comb ($1/l_{my}$ periodicity). So the power spectrum of the global shape is present at each multiple of $1/l_{my}$ (fig. 2.1b).

B. Medium Transfer Function

It can be easily shown that the Fourier transform of the equation (1) is expressed in function of K_0 , the zero-order modified Bessel function of the second kind. The homogeneous medium transfer function is thus expressed by

$$H_h(k) = \frac{1}{4\pi\sigma} K_0(2\pi y k) \quad (3)$$

and represented in the fig. 2 2b.

This transfer function is a low-pass filter, were the slope depends on the depth of the axon. The higher the depth, the higher the filtering. This relation will be shortly analyzed in more detail using a more realistic model.

C. Extracellular AP

As in the space domain the potential is the result of the convolution product between the current and the transfer function, hence in the frequency domain the potential specter equal to the product between the current spectrum and the transfer function.

The figure (2. 3b) presents the extracellular AP spectrum. In this example, the second lobe is around 1000 m^{-1} , and is attenuated 'according to the depth of the axon'. For the shortest distance ($200 \mu\text{m}$), the major part of the power spectrum is present around the low frequencies and around $1/l_{my}$, but for the second signal ($\rho' = 500 \mu\text{m}$) the major part of the power is in the low frequency. This explains that the spikes present on the extracellular AP disappear according to the depth of the axon. It is directly linked to the transfer function behavior. Thus, a study of this transfer function with a more realistic model is needed to quantify this phenomenon.

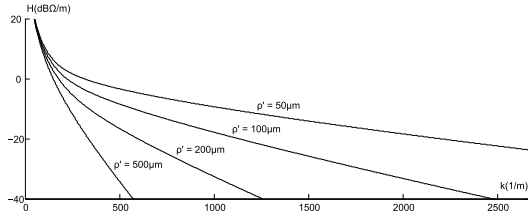


Fig. 3. Spatial transfer function spectrum for the inhomogeneous and anisotropic model for relative distances between the electrode and the axon $\rho' = 50, 100, 200$ and $500 \mu\text{m}$.

TABLE I

MODEL PARAMETERS USED FOR SIMULATIONS AS PRESENTED IN [2]

σ_ρ	$0.1\Omega^{-1}m^{-1}$	conductivity of the fascicle in radial and longitudinal direction
σ_z	$0.5\Omega^{-1}m^{-1}$	conductivity of the perineural sheath
σ_s	$2000\Omega^{-1}m^{-1}$	conductivity of the extraneurium
σ_e	$0.001\Omega^{-1}m^{-1}$	conductivity of the extraneurium
a	$300\mu\text{m}$	radius of the nerve
r		radial position of the fiber
ρ		radial position of the pole

IV. INHOMOGENEOUS MODEL

As said previously, the homogeneous nerve model, although useful, is too simple to provide quantitative data. The analytical work in [2] presents a more realistic nerve model (table I). The model is anisotropic, *i.e.* different fascicle conductivities are defined according to the direction (longitudinal or radial), and inhomogeneous, taking into account the perineural sheath conductivity (σ_s) and the extraneurium conductivity (σ_e). In particular, this extraneurium can represent an insulated cuff. From this model, the authors gives an analytical expression of the extracellular AP using the medium transfer function in the frequency domain

$$H_i(k) = \frac{1}{4\pi^2\sigma_\rho} \sum_n \frac{K_n(k\rho)\cos(n\theta) \cdot (2 - \delta_n)I_n(kr^*)k\sqrt{\sigma_\rho\sigma_z\sigma_s} \cdot (I_n(ka^*)K'_n(ka^*) - I'_n(ka^*)K_n(ka^*))}{(k\sqrt{\sigma_\rho\sigma_z}I'_n(ka^*) + \sigma_s I_n(ka^*))k\sigma_e K'_n(ka) - k\sqrt{\sigma_\rho\sigma_z}\sigma_s I'_n(ka^*)K_n(ka)} \quad (4)$$

with:

- $a^* = a\sqrt{\sigma_z/\sigma_\rho}$,
- $r^* = r\sqrt{\sigma_z/\sigma_\rho}$,
- k spatial plusation (rad m^{-1}),
- I_n the n -order modified Bessel function of the first kind,
- K_n the n -order modified Bessel function of the second kind,
- $\delta_n = 1$ for $n = 0$ and $\delta_n = 0$ for $n \neq 0$.

This equation shows that the transfer function behavior depends on the relative location of the axon inside the nerve and that of the electrode poles (ρ' and θ). The dependance of $H_i(k)$ with ρ' is illustrated by the figure fig. 3 showing the particular case where the poles are placed on the top of the nerve ($\rho = a$) just above the active axon ($\theta = 0$). Compared to the medium transfer function of the homogenous model

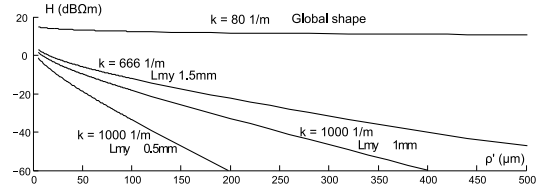


Fig. 4. Behavior of the transfer function according to the distance for spatial frequencies corresponding to global AP shape, and fibers with $l_{\text{my}} = 0.5, 1$ and 1.5 mm .

H_h presented fig. 2, it appears that low frequencies are amplified, whereas the attenuation is higher for high frequencies.

V. HIGH-FREQUENCY ATTENUATION

As explained in the previous part, the high spatial frequency component of the signal is limited to a local phenomenon. Significant power can be present in the second lobe of the spatial spectrum (fig. 2.3b). Because this lobe is centered on a particular frequency for each fiber (corresponding to the NoR periodicity), this section will focus on some frequencies of interest. Based on the study by McIntyre *et al.* [3], we chose $k = 80, 666, 1000$ and 2000 m^{-1} to illustrate respectively the low-frequency global shape and the second lobe for $l_{\text{my}} = 1.5, 1$ and 0.5 mm .

A. Description

The figure 4 presents the values of the transfer function for these frequencies of interest plotted according to the depth (ρ'). Let's focus on the depth $\rho' = 100 \mu\text{m}$. For the low frequency component (80 m^{-1}) the transfer function value is about $13 \text{ dB}\Omega\text{m}$. This means that for a nodal current of amplitude $1 \mu\text{A}/\text{m}$ (this is the typical case for $l_{\text{my}} = 1 \text{ mm}$ and $i_n = 1 \text{ nA}$) the resulting low-frequency AP component is around $13 \text{ dB}\mu\text{V}$ or $4 \mu\text{V}$.

For the highlighted frequencies for the second lobe for $l_{\text{my}} = 0.5, 1$ and 1.5 mm the transfer function value are respectively $-33.06, -17.69$ and $-11.62 \text{ dB}\Omega\text{m}$ (taken as a 0 dB referee in the figure 5). It mean that the high frequencies components are approximately attenuated by $-46, -31$ and $-25 \text{ dB}\Omega\text{m}$ (respectively), compared to the low frequency component. So for this example (distance of $100 \mu\text{m}$) for all span of fiber the high frequencies components amplitude are approximately comprised between $0.02, \text{ and } 0.25 \mu\text{V}$, which is a quite low amplitude.

However it is interesting to pay attention to the attenuation in function of the distance ρ' . This attenuation between is computed between $\rho' = 100 \mu\text{m}$ and $\rho' = 500 \mu\text{m}$). For the low frequency, there is an attenuation of $4.175 \text{ dB}/\text{mm}$ this confirm that the axon location has not a high influence on the transfer function value. But for highlighted frequencies, the attenuation are respectively $260.1, 134.2$ and $87.62 \text{ dB}/\text{mm}$ this confirm that the axon location has a huge influence on the transfer function value.

The figure 4 show a particular case, more generally, the figure 5 is obtain thanking into account all possible location of the axon inside the nerve. This figure represents the pole relative sensitivity equivalues to an active axon. It is

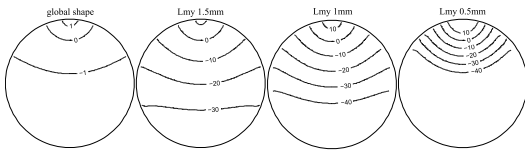


Fig. 5. Pole sensitivity for the spatial frequencies of interest, referenced to the sensitivity at the distance of $100 \mu\text{m}$. $20 * \log(H)$ with H in Ωm . If $i_n = 1 \text{ nA}$ and $H = 0 \text{ dB}\Omega\text{m}$ it gives $V = 1 \mu\text{V}$ amplitude. and for $H = -20 \text{ dB}\Omega\text{m}$ it give $V = 0.1 \mu\text{V}$ amplitude

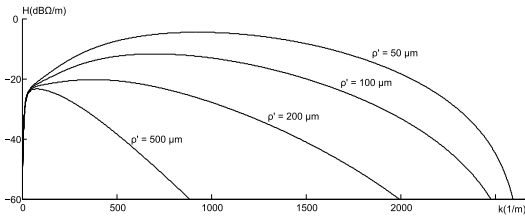


Fig. 6. Global spatial transfer function from the nodal current input to the output of the band-pass filter for distances $\rho' = 50, 100, 200$ and $500 \mu\text{m}$.

compared to the reference value of the transfer function for a distance of $100 \mu\text{m}$ (presented above). The cross views of the nerve correspond to the same four spatial frequencies of interest as before. In this 2-D view it can be see that a pole has a local sensitivity for the high frequencies, even if the sensitivity equivalues are not concentric circles.

B. Extraction

For better selectivity, the electrode has to be sensitive only to high spatial frequencies. We thus propose to use the electrode as a spatial band-pass filter. The classical ENG recording is performed with a tripole having a frequency response expressed by

$$F(k) = 1 - \cos 2\pi kh. \quad (5)$$

We have shown in [4] that setting the longitudinal inter-pole distance (h) to $375 \mu\text{m}$, the band-pass of the filter covers the spatial frequencies corresponding to most of nerve fiber types (666 (m)^{-1} to 2000 (m)^{-1}).

To obtain the global transfer function linking the nodal current to the tripole output, we have to multiply $F(k)$ by the medium transfer function $H_i(k)$. The resulting function is plotted in fig. 6 for different axon depth (ρ'). It clearly appears that the total transfer function also acts as a band-pass filter for the closest distances but more as a low-pass filter for the larger ones.

Because the maximum value of this total transfer function is about 0 dB, we could expect some hundreds of microvolt for the closest actives fiber. So, for a compound AP, we hope that this value could reach some μV and can be measured.

As previously stated, the Laplacian computation must be the first processing of the recorded signal. For this purpose, we propose the use of a modified differential pair. Fig7 shows the principle of the preamplifier. An ASIC with this type of preamplifier stage has been designed (AMS $0.35 \mu\text{m}$ technology) for the multipolar electrode.

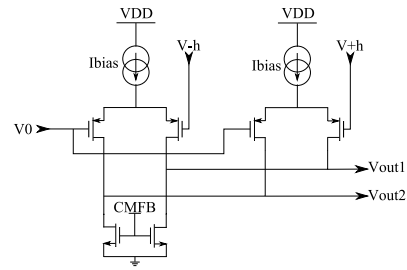


Fig. 7. Three-input preamplifier performing the Laplacian computation.

VI. CONCLUSION

In this paper, thanks to analytical study using an inhomogeneous an anisotropic nerve model, we have described qualitatively and quantitatively the spatial properties of an extracellular AP. Using the spectral analysis on this spatial signal, first we have shown that high spatial frequencies component exist on an extracellular AP and are related to the type of fibers. Then we described that there is specific attenuation related to the distance. As a result this high frequency component appear as a local phenomenon. The aim of this study is to propose an spatial selective electrode. We propose a spatial filtering based on electrode design and an electronic architecture to extract this phenomenon. He have proposed an electrode design a far more selective than usual.

The drawback is that the local phenomenon signal extracted by the proposed electrode is around μV . This implies the use of low-noise and high-gain amplification electronics to exploit this electrode design. Unfortunately, due to small pole diameter ($\approx 100 \mu\text{m}$), expected electrochemical noise will be of the same range as the measurable signal with usual electrode materials. As the expected SNR is very low, more accurate studies have to be realized to ensure the feasibility of this new approach.

Of course, we also show that the very weak expected amplitude raises several technological deadlocks that need to be overcome before actual applications. However, a first experimental proof of concept is planned thanks to an *artificial* axon allowing the nodal currents to be increased for several orders of magnitude to get rid of the SNR limitation.

REFERENCES

- [1] M. Djilas, C. Azevedo-Coste, D. Guiraud, and K. Yoshida, "Interpretation of muscle spindle afferent nerve response to passive muscle stretch recorded with thin-film longitudinal intrafascicular electrodes," *IEEE Transactions On Neural Systems And Rehabilitation Engineering*, vol. 17, no. 5, pp. 445–453, 2009.
- [2] J. H. Meier, W. L. Rutten, and H. B. Boom, "Extracellular potentials from active myelinated fibers inside insulated and noninsulated peripheral nerve." *IEEE transactions on bio-medical engineering*, vol. 45, no. 9, pp. 1146–53, Sep. 1998. [Online]. Available: <http://www.ncbi.nlm.nih.gov/pubmed/9735564>
- [3] C. C. McIntyre, A. G. Richardson, and W. M. Grill, "Modeling the excitability of mammalian nerve fibers: Influence of afterpotentials on the recovery cycle," *Journal of Neurophysiology*, vol. 87, pp. 995–1006, february 2002.
- [4] O. Rossel, F. Soulier, S. Bernard, and G. Cathébras, "New electrode layout for internal selectivity of nerves," in *EMBC'09: 31st Annual International Conference of the IEEE Engineering in Medicine and Biological Society*, 2009.